16th Australasian Wind Engineering Society Workshop
Brisbane, Australia
18-19 July, 2013

Distribution of wind loads in a roof system and fragility analysis

Chana Jayasinghe[1], John Ginger[1], David Henderson[1] and George Walker[1]
[1]Cyclone Testing Station, School of Engineering and Physical Sciences,
James Cook University, Townsville, Australia

Abstract

This paper investigates the transmission of wind loads through a roofing system of contemporary houses built in Australia. The distribution of wind loads and associated structural response of batten-to-truss connections including the effect of failures is investigated. The study found that the use of normal design practices can significantly underestimate connection loads, when highly correlated wind pressures act on the roof. A process for assessing the fragility of roof components to wind loads is proposed. The fragility of components can be incorporated to develop vulnerability functions for these contemporary houses.

Introduction

Increasing concentrations of population combined with increasing real wealth is creating concern about the increasing magnitude of the economic losses from disasters arising from major events like tropical cyclones. An approach called performance based design (PBD) is being developed to overcome the limitation in current design which only focuses on the structural safety of individual buildings (Walker, 2011). In respect of wind design this approach requires information on the relationship between wind speeds and the cost of damage for a building, which is described as its vulnerability to wind. Although full-scale tests, such as those by Boughton and Reardon (1984), provide data on the overall performance under specific conditions they are limited in terms of general application. For general application an analytical procedure based on an understanding of the relationship between damage and wind speeds for individual components and sub-systems, known as fragility analysis, is required. This paper describes an investigation of the fragility of a metal clad roofing system. It is primarily a summary of work undertaken by Jayasinghe (2012).

The investigation focused on the batten-to-truss connection of a metal clad roof supported by battens attached to roof trusses typical of a system used on many houses in Australia. The investigation comprised three phases: 1) Measurements of the wind pressures on the cladding, 2) Analysis of the transmission of loads from the cladding to the batten-to-truss connections, and 3) Analysis of the fragility of the system assuming no loss of strength due to fatigue.

Roof structure, loads and response

A survey conducted in the cyclonic region of North Queensland in 2008-10, found that more than 90% of the contemporary houses being built were masonry block type. Jayasinghe (2012) described the common, contemporary gable-end house and defined the structural systems used. Jayasinghe and Ginger (2011) obtained external pressures on parts of the roof from a wind tunnel model of a representative contemporary house, and also presented these wind pressures in probabilistic form. They confirmed that the wind loads at the gable end and corners of the roof are larger compared to the middle region, and that AS/NZS 1170.2 (2011) underestimates the external pressures on cladding fixings near the ridge at the gable roof edge, but gives reasonable estimate for the pressures on other areas.

This section describes wind load near the gable end of a common contemporary house roof and the structural (i.e. batten-to-truss connections) response of the roof segment comprising batten-to-truss connections A5 to A8, B5 to B8, C5 to C8 and D5 to D8 of trusses A, B, C and D, shown in Figure 1. Truss A is at the gable-end. The spatial and temporal distribution of pressures is obtained for wind approach directions around the compass from the wind tunnel model study, and the peak loads on these batten-to-truss connections are derived from the pressure measurements on this part of roof, and structural tests.

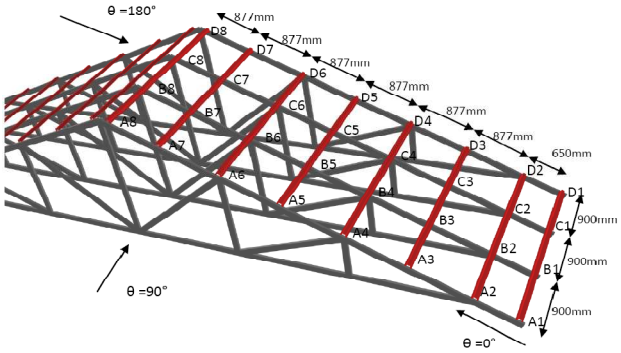

Figure 1. Schematic Diagram of roof structure

The structural response was studied by conducting a series of tests on a roof system with 90mm × 35mm, MGP 12 top chord truss elements, and 40 mm × 40mm, BMT 0.75mm top-hat battens and BMT 0.42mm corrugated roof cladding, shown in Figure 2. Common spacings were used for battens, trusses and for cladding fixings in this representative roof system. The battens were fixed to the truss elements via tension/compression 'S' type load cells at batten-to-truss connections. The roof cladding was fixed to the battens with Type-17 cladding fasteners (No14-10 × 50mm) at the crests of alternate corrugations, as shown in Figure 2. The applied load and load on connections were measured with 'S' type load cells. Loads were applied on the bottom surface of the roof cladding using a jack. Timber blocks and foam moulds were shaped to match the profiles of the battens or the cladding at the locations of load application.

Figure 2. Roof test set up

The time, t varying load at a connection (cladding fixing or batten-to-truss ($X_b(t)$) is given by;

$$X_b(t) = \left(\sum_{i=1}^{N} \beta_i A_i C_{p_i}(t)\right) \times {}^1/_2 \rho \bar{U}_h^2 \quad (1)$$

where,
β_i-Reaction coefficient for load applied at pressure tap location, i
A_i- Tributary area for pressure tap, i
$C_{p_i}(t)$ -Pressure coefficient at pressure tap, i at time t
ρ – Density of air
$\bar{U}_h$ - Mean wind speed at mid roof height
N- Number of pressure taps affecting on the connection being considered.

The reaction coefficients were obtained for various (i.e. elastic, plastic, and selected cladding fastener and batten-to-truss connection failure) scenarios by dividing the load at each batten-to-truss connection with the load applied at location i.

The load acting on the batten-to-truss connection is represented in coefficient form shown in Equation 2. Here, A_N is the nominal area related to batten-to-truss connections taken as 0.9 × 0.9 = 0.81m^2. The external pressure coefficients are used in the analysis and a negative value of C_{X_b}represents an uplift load on the connections.

$$C_{X_b}(t) = \frac{X_b(t)}{\frac{1}{2}\rho \bar{U}_h^2 . A_N} = \frac{\sum_{i=1}^{N} \beta_i A_i C_{p_i}(t)}{A_N} \quad (2)$$

Applying the nominal peak pressure coefficients from AS/NZS1170.2, $C_{p_N} = C_{p_e} \times K_l \times G_U^2$, where C_{p_e} = -0.9 is the external pressure coefficient, K_l =1.5 is the local pressure factor, and $G_U = \hat{U}_h/\bar{U}_h$ = 1.875 is the velocity gust factor, where, $\hat{U}_h$ and $\bar{U}_h$ are gust and mean wind speed respectively at mid roof height, gives peak value of C_{X_b}, $\check{C}_{X_b}$ = -4.75.

The structural tests by Jayasinghe (2012) indicated that the wind pressure on the shaded area shown in Figure 3 has a significant influence on the load at connection, B7. Thus, the pressure acting on the adjoining panels (outside the conventional tributary area used) must be considered when determining the load acting on a batten-to-truss connection. Jayasinghe et al (2012) used this method which accommodates the load distribution effects with spatially and time varying wind pressure to derive the peak load (i.e. $\check{X}_b$) of each connection by combining reaction coefficients with the simultaneous measurement of wind pressure on each pressure tap (using Equation 1) for each wind approach direction.

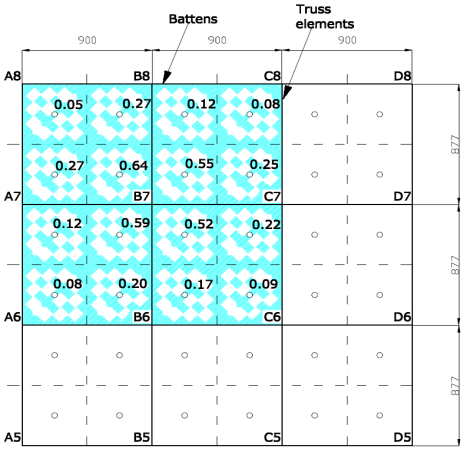

Figure 3. Tributary area influencing the load on B7, with load distribution effects, Note: o- Pressure taps, the values shows next to the pressure taps are reaction coefficients

Figure 4 shows the variation of load on the connection B7 in terms of mean and peak values with the wind approach direction. As shown in the Figure 4, connection B7 experiences large loads for wind approach directions 135° to 150°, and the maximum load, $\check{C}_{X_b}$ of -5.12 occurs at 150°. Connection at B7 was the most critical connection for wind approach direction 150°. Table 1 shows the load distribution on connections calculated using this method in terms of $\check{C}_{X_b}$ for 150° wind approach direction (i.e. wind direction that generated the largest load effect). The load distributions for other directions were also determined in similar manner.

Table 1. $\check{C}_{X_b}$ for θ =150°- Undamaged roof using load distribution effects

Connection Number	$\check{C}_{X_b}$		
	Truss A	Truss B	Truss C
5	-2.45	-3.84	-2.69
6	-3.18	-3.99	-3.18
7	-3.86	**-5.12**	-4.59
8	-2.54	-4.44	-3.72

Figure 5 is the instantaneous pressure pattern responsible for generating this peak load. The well correlated large negative pressure resulting from edge vortices formed on and outside the conventional tributary and the flexibility of the roof (shown by the reaction coefficients) contributes to the high load at the connection. Jayasinghe (2012) showed that methods using conventional tributaries can significantly underestimate the load on some batten-to-truss connections.

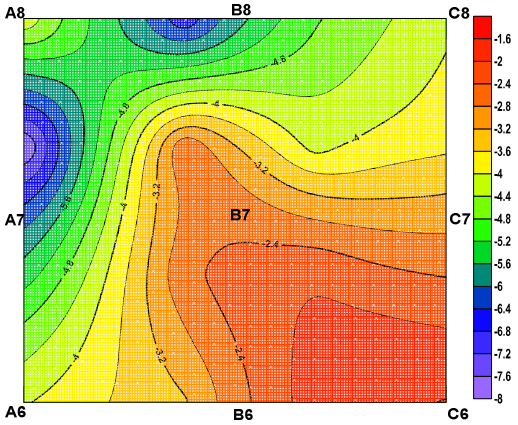

Figure 5. Pressure (Cp) distribution generating peak load at B7

Henderson (2010) showed that the wind load measured by a single pressure tap located on the conventional tributary area of a cladding fastener can be used to satisfactorily represent the load on a fastener, and analyze its response.

Load re-distribution following fixing failures

The redistribution of loads to batten-to-truss connections in this heavily loaded roof edge region for wind direction 150^o following the failure of a cladding fixing or a batten-to-truss connection is given in Tables 2 and 3 respectively. The failure of a cladding fixing (on Batten #7) will redistribute the loads to the fasteners on either side along the stiff corrugation to battens B6 and B8. The failure of batten-to-truss connection B7 will transfer most of the load to B6, C7 and A7.

Table 2. $\check{C}_{X_b}$ for θ =150°- Cladding fastener failure (between B7 and C7)

Connection Number	$\check{C}_{X_b}$		
	Truss A	Truss B	Truss C
5	-2.45	-3.84	-2.69
6	-3.18	-4.44	-3.30
7	-3.86	-4.49	-4.35
8	-2.54	**-4.70**	-3.85

Table 3. $\check{C}_{X_b}$ for θ =150°- Batten-to-truss connection B7 failed

Connection Number	$\check{C}_{X_b}$		
	Truss A	Truss B	Truss C
5	-2.45	-3.84	-2.69
6	-3.18	-5.27	-3.18
7	-5.09		**-6.64**
8	-2.54	-4.55	-3.72

Fragility Analysis

The load distributions discussed in the previous section were obtained by applying deterministic (patch) loads and obtaining loads on connections. The assessment of component fragility and development of vulnerability models require these parameters to be analysed in a probabilistic manner.

The failure of a connection is defined when the wind load combined with dead load exceeds the capacity of the connection. The probability of failure of roofing components is determined with increasing wind speed. The wind load acting on a batten-truss connection can be obtained in probabilistic form with the variables in Equation 3. For wind uplift, the limit state of each connection is expressed as shown in Equation 4.

$$W = {}^{1}/_{2}\,\rho V^2 \times C_{x_b} \times A_N \qquad (3)$$

$$R\text{- }(W\text{-}D) = 0 \qquad (4)$$

Here, *R*- Strength (i.e. capacity) of the connection, *D*-Dead load and *V*- is the gust wind speed at 10m height.

Failure occurs when $R\text{- }(W\text{-}D) < 0$.

The connection strengths are given in Jayasinghe (2012), and the fragility of selected batten-to-truss connections are assessed using Equations 3 and 4. The probability of failure of connections (i.e. fragility) is calculated for increasing steps of wind speeds by repeating the reliability analysis described by Jayasinghe (2012), at each wind speed increment.

The passage of a cyclone would generate a complex loading regime on parts of a roof, as described by Jancauskas *et al.* (1994). Changes in wind direction will occur in addition to progressively increasing speeds that reach a maximum and then drop-off, depending on the orientation of the house to the track of the cyclone. A detailed fragility assessment requires a comprehensive analysis of load cycles and fatigue response of the connections. The analysis that follows in this section, provides a basis for this assessment by estimating the relative fragility (i.e. probability of failure) of batten-truss connections on the part of the roof for given wind approach directions.

Figure 6 shows the probability of failure of batten-to-truss connections B6, B7, B8, A7 and C7 by incorporating the load distribution effects for 150° wind approach direction. Connection B7 was the most vulnerable connection. This analysis assumed zero internal pressure, and that cladding fasteners have not failed.

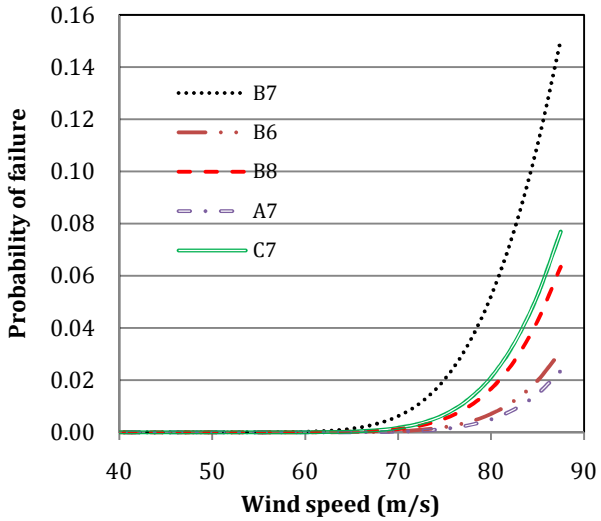

Figure 6. Vulnerability of batten connections for θ=150°

Failure of a door or a window can create a dominant opening in leading to a significant increase in internal pressure. Jayasinghe (2012) studied the effect of internal pressure coefficients 0.2, 0.4 and 0.7(from AS/NZS1170.2). Figure 7 shows the fragility of batten-to-truss connections using internal pressure coefficient of 0.7 applied for each wind speed step in this analysis, for wind approach direction of 150°. Figure 7 shows, connection B7 is still the most vulnerable and at a wind speed of 75m/s, the probability of failure of connection B7 has increased up to 25%. However, the changing wind direction during the passage of a cyclone will reduce the damage (i.e. the probability of failure).

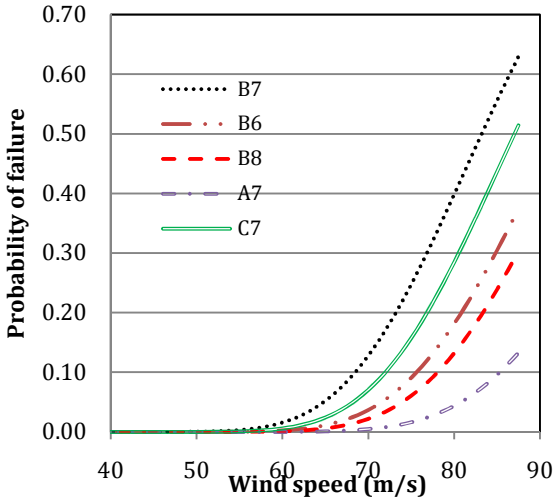

Figure 7. Vulnerability of batten connections for θ=150° - internal pressure coefficient +0.7

Figure 8 shows the fragility of connections B6, B8, A7 and C7 in the roof with a failed connection B7, for 150° wind approach direction, for internal pressure = 0. The results reflect the data in Table 3, which shows the connection C7 becomes more vulnerable. For example, the probability of failure of C7 increases from 1% (from Figure 6) to 11% at 75m/s. Thus, the load distribution effects must be incorporated when determining the vulnerability of these connections.

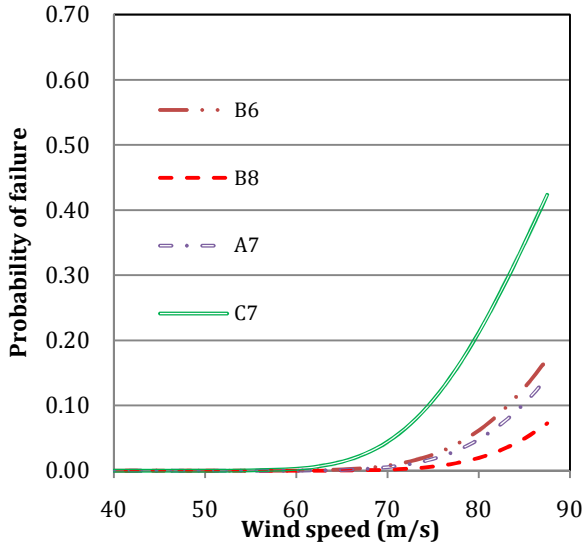

Figure 8. Probability of batten-truss connection failure vs wind speed following the failure of B7 - internal pressure coefficient- 0

However, the application of this test data for a population of houses that are located in the community requires consideration of parameters such as those defined in wind load probabilistic model and the directional variability of wind pressure during a cyclone (Jancauskas *et al.* (1994)). Such an analysis will also need to account for variation in house geometry, internal pressure, terrain, topography and shielding in addition to the variation in batten and truss layouts and fixings. Jayasinghe (2012) indicated that these factors have a significant impact on the connection vulnerability and should be used for assessing the overall vulnerability of the houses.

Conclusions

This paper discuses the transmission of wind load effects through the roof of contemporary houses built in the cyclonic region of Australia focusing on the batten-truss connection. This is a summary of the work by Jayasinghe (2012).

The main conclusion drawn from this study is that loads on the batten-to-truss connections are strongly influenced by the behaviour of the structural system and the wind pressure distribution on the roof. The study showed that load transferred to batten-truss connections are influenced by the flexibility of the battens and cladding used in the roof, and the directional stiffness characteristics of the cladding. Furthermore, these connection loads are dependent on the instantaneous spatial distributions of the wind pressure on the cladding supported by these fixings. As a result, estimates based on the application of wind pressures to conventional connection tributary areas, which is normal design practice, can be unreliable and lead to underestimation of connection loads. The study showed that a larger area of load influence should be considered when calculating the batten-to-truss connection loads on these roof structural systems. A primary outcome of this study is the establishment of an improved procedure for analysing the variation of the connection loads with time, taking account of the spatial and temporal variation in wind pressures and the structural response characteristics of the roof system, which is a necessary step in the assessment of the fragility of roof components and the vulnerability of houses.

References

Boughton, G. N. and Reardon, G. F. (1984) Simulated Wind Load Tests on the Tongan Hurricane House, Cyclone Testing Station, James Cook University, Townsville, TR 23.

Henderson, D. J. (2010) Response of pierced fixed metal roof cladding to fluctuating wind loads. PhD Thesis, James Cook University, Townsville.

Jancauskas, E. D., Mahendran, M. and Walker, G. R. (1994) Computer simulation of the fatigue behaviour of roof cladding during the passage of a tropical cyclone. Journal of Wind Engineering and Industrial Aerodynamics 51(2): 215-227.

Jayasinghe, N. C. (2012) The distribution of wind loads and vulnerability of metal clad roofing structures in contemporary Australian houses. PhD Thesis, James Cook University, Townsville.

Jayasinghe, N. C. and Ginger, J. D. (2011) Vulnerability of Roofing Components to Wind Loads. Wind & Structures 14(4): 321-335.

Jayasinghe, N. C., Ginger, J. D., Henderson, D. J., and Walker, G. R. (2012) Distribution of wind loads in roofing connections. Proceedings ASEC12, 11-13 July 2012, Perth, WA, Australia

Standards Australia. (2011) AS/NZS 1170.2. Structural Design Action Part 2:Wind Action. Standard Australia, Sydney, NSW.

Walker, G.R. (2011)., Modelling the vulnerability of buildings to wind – a review. Canadian Journal of Civil Engineering. 38:9, 1031-1039.

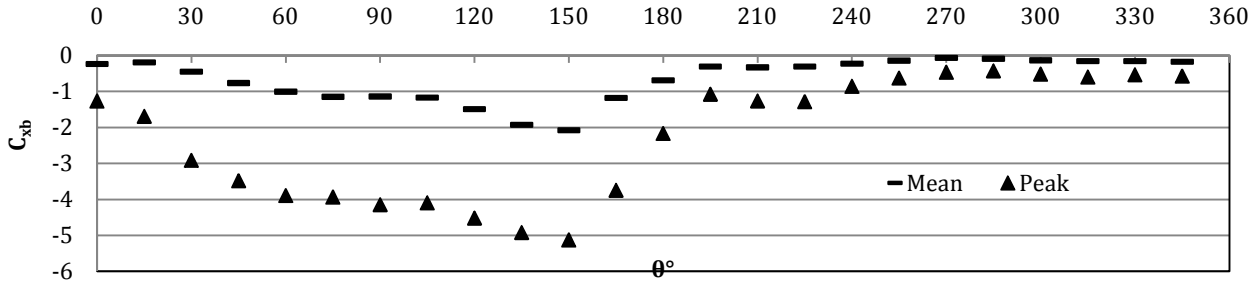

Figure 4: Variation of C_{X_b} at B7 with the wind approach direction

***A summary of this paper is submitted as an Abstract to APCWE-8**